Efficient activation of p53 pathway in A549 cells exposed to L2, a novel compound targeting p53–MDM2 interaction

Lei Zhang[a], Jun Zhang[a], Chunqi Hu[b], Ji Cao[a], Xinglu Zhou[a], Yongzhou Hu[b], Qiaojun He[a] and Bo Yang[a]

The tumor suppressor p53 plays a key role in the regulation of cell cycle, apoptosis, DNA repair, and senescence. It acts as a transcriptional factor, and is able to activate various genes to exert specific functions. MDM2, the main regulator of p53, inhibits the function of p53 through direct interaction. On the basis of this finding, inhibiting the MDM2–p53 interaction can be a potentially important target for cancer therapy. We showed here that L2, an analog of small-molecule MDM2 antagonist nutlins, stabilized p53 and selectively activated the p53 pathway in *p53* wild-type A549 cells, resulting in a pronounced antiproliferation effect through inducing cell cycle arrest and apoptosis. Meanwhile, we confirmed by immunoprecipitation analysis that L2 could also inhibit MDM2–p53 interaction, similar to nutlin-1. Real-time PCR results revealed that L2 had no effect on the *p53* gene transcriptional level, but it could induce the upregulation of p21 at the transcriptional level, which was the downstream of p53. Therefore, we concluded that the accumulation of p53 caused by L2 was mainly because of the decrease of the protein degradation rather than the elevation of *p53* gene expression. Furthermore, no phosphor-p53 formed after L2 treatments, indicating that a genetoxic mechanism was unlikely to contribute to the activation of p53 by L2. In conclusion, the data acquired from A549 cells indicated that L2 exhibited high antiproliferation activity by disrupting MDM2–p53 interaction, and that the mechanism was derived from the activation of p53 and the p53 pathway. It was also surprising that L2 showed high antiproliferation effect against *p53* null HL60 cells, which was quite different from nutlin-1. G_2/M phase arrest might have contributed to the high antiproliferation activity of L2 on HL60 cells. The changes of p53 and MDM2 protein levels in L2-treated HL60 cells indicated that the mechanisms involved in the cell cycle arrest in A549 and HL60 cells were probably different, to which our future research would be devoted. *Anti-Cancer Drugs* 20:416–424 © 2009 Wolters Kluwer Health | Lippincott Williams & Wilkins.

Anti-Cancer Drugs 2009, **20**:416–424

Keywords: apoptosis, cell cycle arrest, MDM2, p53

[a]Institute of Pharmacology and Toxicology and [b]Zhejiang University-Ecole Normole Superienre Joint Laboratory of Medicinal Chemistry, College of Pharmaceutical Sciences, Zhejiang University, Hangzhou, Zhejiang, China

Correspondence to Dr Bo Yang and Dr Qiaojun He, Institute of Pharmacology and Toxicology, College of Pharmaceutical Sciences, Zhejiang University, 388# Yuhangtang Road, Hangzhou, Zhejiang 310058, China
Tel/fax: +86 571 88208400; e-mail: yang924@zju.edu.cn; qiaojunhe@zju.edu.cn

Received 14 October 2008 **Revised form accepted** 20 February 2009

Introduction

The p53 tumor suppressor is a principal transcriptional factor mediating cell growth arrest, senescence, and apoptosis in response to a large degree of cellular damage [1]. It has been reported that p53 maintains a very low level in normal cells [2]. Stresses, such as hypoxia or DNA damage, cause p53 to accumulate in the nucleus, where it can exert its transcriptional function [2,3]. The important role of p53 suggests that the loss of p53 may cause dramatic consequences. In humans, about 50% of tumors are thought to obtain mutated *p53*, and in some tumor types, these mutations are associated with poor prognosis and treatment failure [4,5].

The loss of *p53* is not the only way to inactivate p53 in tumors. It can also be the consequence of overexpressing the MDM2 protein [6]. During the past decade, MDM2 has emerged as the principal cellular antagonist of p53 by limiting the tumor suppressor function of p53 through direct interaction, which contributes to the unstable property of p53 in normal unstressed cells [6,7]. MDM2 overexpression correlates with poor prognosis in some tumors, resulting from its inhibition of p53 function and other tumor suppressor proteins. Interestingly, MDM2 itself is the product of a *p53*-inducible gene [8]. Thus, the two molecules are closely linked to each other through an autoregulatory negative feedback loop. MDM2 is transcriptionally activated by p53 and, in turn, inhibits p53 activity by inhibiting its transcriptional activity, mediating its export and increasing its degradation as its E3 ligase [8,9]. In addition, MDM2 has been shown to interact with a large number of cellular proteins besides p53 [10,11]. Although the exact functions and significance of these interactions are not fully understood, the p53-independent functions of MDM2 may also be essential in cancer etiology and progression [10,11].

The design of compounds disrupting the interaction between p53 and MDM2 is therefore an attractive strategy for activating tumor suppressor p53 in tumors. Based on this, the scientists at Roche (Basel, Switzerland) have already identified a series of potent and selective

 DOI: 10.1097/CAD.0b013e32832aa7b0

small-molecule antagonists of MDM2 named nutlins and confirmed their mode of action through the crystal structures of the complex [12]. They confirmed that nutlins could activate the p53 pathway in cancer cells, leading to growth arrest, apoptosis, and growth inhibition of human tumor xenografts in nude mice, but the inducing apoptosis activity of nutlins was not so satisfying [12,13]. Here, we present an analog of nutlins that showed higher antitumor and selective activity compared with nutlins; and the studies of the mechanisms on its antitumor activity could shed light on the significance of the clinical application of these compounds.

Materials and methods

Drugs and chemicals

L2 was supplied by Professor Yongzhou Hu. The structures of L2 were determined by infrared spectrophotometry, mass spectrometry, and nuclear magnetic resonance; the purity of L2 was greater than 95%. The stock solution of L2 (40 mmol/l) was prepared with dimethyl sulfoxide (DMSO) and stored at $-20^{\circ}C$ for in-vitro tests. The stock solution was further diluted with the appropriate assay medium immediately before use. The final DMSO concentration did not exceed 0.1% throughout the study. Antibodies for p53, MDM2, p21, Cdc2, cyclinB, CDK2, cyclinE, Bax, Bcl-2, caspase3, XIAP, phosphor-p53 (Ser^{20}), β-actin, and LaminB were purchased from Santa Cruz Biotechnology (Santa Cruz, California, USA). The horseradish peroxide-labeled secondary anti-goat, anti-mouse, and anti-rabbit antibodies were also purchased from Santa Cruz Biotechnology. Western blot detection reagent, ECL, was purchased from Pierce Biotechnology (Rockford, Illinois, USA). The 5-(and-6)-carboxy-2′,7′-dichlorofluorescin diacetate (carboxy-DCFDA) was purchased from Molecular Probes (Eugene, Oregon, USA).

Cell lines and cell culture

All cell lines (A549, HCT116, KB, PC3 and HL60) were purchased from Cell Bank of China Science Academy (Shanghai, China). All the cell lines were maintained in RPMI-1640 medium (Gibco, Grand Island, New York, USA) plus 10% heat-inactivated fetal bovine serum and incubated at 37°C in a 5% CO_2 atmosphere. Penicillin (100 U/ml) and streptomycin (100 U/ml) were added in the medium.

Cell viability assay

A549, HCT116, KB, PC3, and HL60 cells were plated in 96-well plates (4×10^3/well) for 24 h, and subsequently treated with different concentrations of L2 for 72 h. Viable cells were determined by using MTT assay. An MTT solution (5.0 mg/ml in RPMI-1640, Sigma, St Louis, Missouri, USA) was added (10.0 μl/well), and the plates were incubated for another 4 h at 37°C. The purple formazan crystals were dissolved in 100 μl of DMSO. The plates were then read on an automated microplate spectrophotometer (Thermo Multiskan Spectrum, Thermo Electron Corporation, Vantaa, Finland) at 570 nm. The concentration of inhibition for 50% cells of the drug (IC_{50}) was calculated using the software of Dose-Effect Analysis with Microcomputers (Elsevier-Biosoft, Cambridge, UK).

Immunoprecipitation analysis

A549 cells were harvested and 100 μl of the lysis buffer per sample was added. The cells were incubated on ice, and were mixed every 3–5 min. The cells were centrifuged and the supernatant was transferred to a new tube. One microliter of normal IgG and 20 μl protein A/G plus agarose per sample were added and incubated for 30 min on ice and then centrifuged. The supernatant was dislodged to quantitate the protein. Eight micrograms of antibody per 0.5–1 mg protein were added, incubated for 1–2 h and then 20 μl protein A/G plus agarose were added for another 1–2 h, centrifuged, and the precipitation was washed more than five times. The remaining steps were as the same as in the western blot analysis.

Western blot analysis

The protein samples of A549 and HL60 cells were extracted in the lysate buffer consisting of 50.0 mmol/l NaCl, 50.0 mmol/l Tris–HCl, 1.0% Triton X-100, 1.0% sodium deoxycholate, and 0.1% SDS. Total protein concentrations of whole-cell lysates were determined using BioRad BCA method (Pierce Biotechnology, Rockford, Illinois, USA). Total proteins (40.0–80.0 μg) were loaded per lane and fractionated on 10–15% Tris–glycine precast gels, transferred to PVDF membranes (Millipore, Bedford, Massachusetts, USA), and probed with primary antibodies and then with horseradish peroxide-labeled secondary antibodies. Proteins were visualized using ECL.

Fluorescence microscopy

A549 cells were cultured in 6-well plates and treated with or without L2 (12 μmol/l) for 48 h. Cells were washed twice with PBS and fixed with 4% paraformaldehyde, permeabilized with 0.1% Triton X-100. The cells were then incubated overnight with anti-p53 antibody that was diluted to 1 : 60 in PBS containing 3% fetal bovine serum and 1% bovine serum albumin at 4°C. After washing twice with PBS, the cells were incubated with fluorescein isothiocyanate (FITC)-conjugated secondary anti-rabbit antibody staining (1 : 100 dilution) for 1 h at room temperature. The cells were then incubated with DAPI (4′,6-diamidino-2-phenylindole) for 5 min. After washing three times with PBS, the stained cells and nuclei were observed under a fluorescence microscope.

Real-time PCR analysis for p53 and p21 mRNA levels

Total RNA of A549 cells was extracted by Trizol reagent (Bio Basic Inc., Markham, Ontario, Canada) and cDNA was synthesized using 2 μg of the total RNA with random hexamer primers and RevertAid M-MuLV Reverse Transcriptase (Fermentas International Inc., Burlington, Ontario, Canada). The conditions used for reverse-transcription PCR were as follows: 10 min at 25°C, 60 min at 48°C, 15 min at 72°C, and 10 min at 95°C. Typically, 100 ng of reverse-transcribed cDNA per sample were used to perform real-time PCR analysis by QuantiTect SYBR Green PCR kits (Qiagen Inc., Valencia, California, USA). The housekeeping gene *GAPDH* was used as an internal standard. The real-time PCR protocol consisted of thermal cycling as follows: initial denaturation at 95°C for 30 s, 58°C for 30 s, and 72°C for 30 s using an Eppendorf epGradient Mastercycler (Eppendorf, Hamburg, Germany). The primers used for the experiment were as follows: p53, forward: 5′-ACCAGGGCAG CTACGGTTTC-3′, reverse: 5′-CCTGGGCATCCTTGAG TTCC-3′ [14]; p21, forward: 5′-GCGATGGAACTTCGA CTTTGT-3′, reverse: 5′-GGGCTTCCTCTTGGAGAAGA T-3′ [15]; GAPDH, forward: 5′-CCTGGCCAAGGTCATC-CATG-3′ and reverse: 5′-TGAGGTCCACCCTGTTG-3′ [14]. In all experiments, two negative controls were carried through all steps. Values were expressed as fold increase relative to the reference sample.

Cell cycle assay

The cells treated with L2 were collected and washed twice with PBS, and then fixed with 75% alcohol overnight. Then, the cells were washed with PBS and resuspended in PBS. RNase was added for 30 min to eliminate the interference of RNA and then propidium iodide (PI; Sigma) was added for 30 min. Then, the cells were washed and the DNA content was detected by the FACSCalibur (Becton Dickinson, Lincoln Park, New Jersey, USA).

Apoptosis assay

Apoptosis caused by L2 in A549 cells was analyzed by Annexin–FITC/PI apoptosis detection kit (BioVision, Mountain View, California, USA) and flow cytometry.

DAPI staining assay

A549 cells were cultured in 6-well plates and treated with 12 μmol/l L2 for 48 h. The cells were washed twice with PBS and then incubated with DAPI, which was diluted with 0.1% Triton X-100, for 5 min. Cell nucleus was observed under fluorescence microscope.

Detection of intracellular reactive oxygen species content

The production of intracellular reactive oxygen species (ROS) in the A549 cells was measured by the oxidation-sensitive fluorescent dye carboxy-DCFDA. Harvested cells were treated with L2, washed twice with PBS, and then carboxy-DCFDA was added at a final concentration of 15 μmol/l. The cells were incubated at 37°C for an additional 30 min, after being washed twice with PBS and green fluorescence intensity was measured by the FACSCalibur.

Statistical analysis

The values for all the samples in different experimental conditions were averaged and the SD of the mean was calculated. The significance levels were set at a *P* value of 0.05.

Results

The effect of L2 on cell viability

We examined the antiproliferation effect of L2 on five panels of cancer cell lines, two (A549 and HCT116) with wild-type *p53*, three (KB, PC3 and HL60) with mutated or deleted *p53*. These five cell lines were incubated with L2 for 72 h and their cell mass and viability were measured with the MTT assay. Except HL60 cells, a clear separation activity of L2 was observed. Pronounced dose-dependent decreases of cell viability were found in A549 and HCT116 cells after L2 treatments, and reductions in cell viability after 72 h of incubation with 20 μmol/l were 87.42 and 83.59%, respectively. The other two cell lines with *p53* mutated or deleted displayed moderate decreases in cell viability throughout the whole range of tested L2 concentrations; PC3 cells did not even respond to almost all concentrations (Fig. 1b). The IC_{50} values of A549, HCT116, KB, and PC3 cells were 7.68 ± 1.05, 6.37 ± 0.76, 16.69 ± 2.72, and 39.66 ± 5.65 μmol/l, respectively. As

Fig. 1

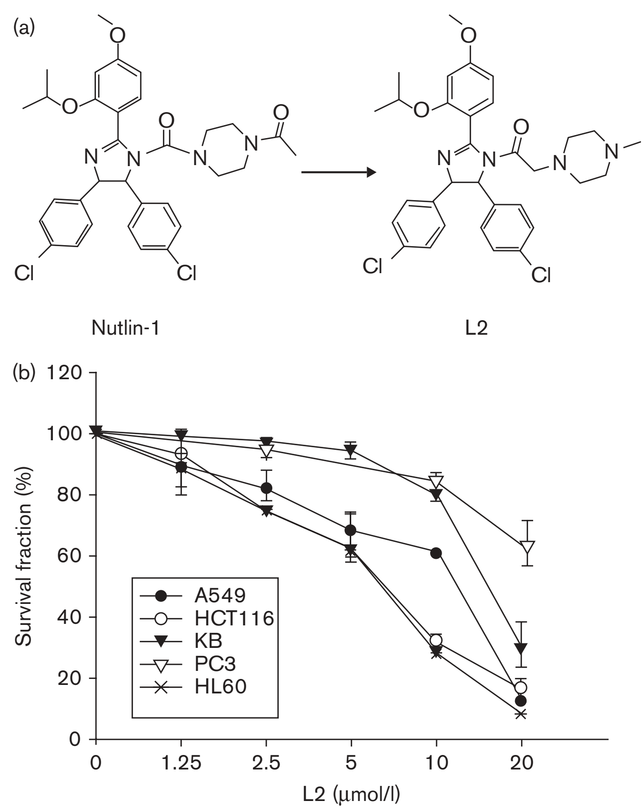

Antiproliferation activity of L2 on several human carcinoma cell lines with different *p53* status. (a) Structures of compounds nutlin-1 and L2. (b) Exponentially growing cancer cells with wild-type *p53* (A549, HCT116), mutated or deleted *p53* (KB, PC3, and HL60) were incubated with various of concentrations (0–20 μmol/l) of L2 for 72 h and the cell mass and viability were measured by the MTT assay.

shown in Table 1, L2 showed a high antiproliferation effect on HL60 cells, which was different from nutlin-1, the IC_{50} value of HL60 cells treated with L2 was 5.26 ± 0.37 μmol/l. It could be concluded that the antitumor activity of L2 was not as largely dependent on the *p53* status as nutlin-1.

Table 1 The IC_{50} values of L2 and nutlin-1 on several different cell lines

Original tumor type	Cell line	IC_{50} (mean ± SD) (μmol/l) L2	IC_{50} (mean ± SD) (μmol/l) Nutlin-1
Non-small-cell lung cancer	A549	7.68 ± 1.05	11.12 ± 0.04
Colon carcinoma	HCT116	6.37 ± 0.76	10.76 ± 0.37
Oral carcinoma	KB	16.69 ± 2.72	17.80 ± 0.24
Androgen-independent prostate cancer	PC3	39.66 ± 5.65	19.18 ± 1.17
Acute myeloid leukemia	HL60	5.26 ± 0.37	13.56 ± 0.71

IC_{50}, half maximal inhibitory concentration.

L2 disrupted MDM2–p53 interaction, stabilized *p53* and *p53*-targeted genes in A549 cells

As an analog of nutlins, we intended to examine whether L2 could also disrupt MDM2–p53 interaction. A549 cells were treated with 8 and 16 μmol/l of L2 or 16 μmol/l of nutlin-1 for 48 h. Immunoprecipitation results showed that MDM2 protein, which coimmunoprecipitated with p53, decreased in a dose-dependent manner, and a similar inhibition was induced by the equivalent amount of nutlin-1 and L2 (16 μmol/l) (Fig. 2a). According to the model for p53 regulation by MDM2, the treatment of cells with inhibitor of MDM2–p53 binding was supposed to result in the accumulation of the p53 protein and activation of the p53 pathway. In line with this assumption, we first examined the effects of L2 on the cellular levels of p53 and its targeted proteins. The protein levels of p53, MDM2, and p21 were elevated in a dose-dependent manner after exposure of A549 cells to

Fig. 2

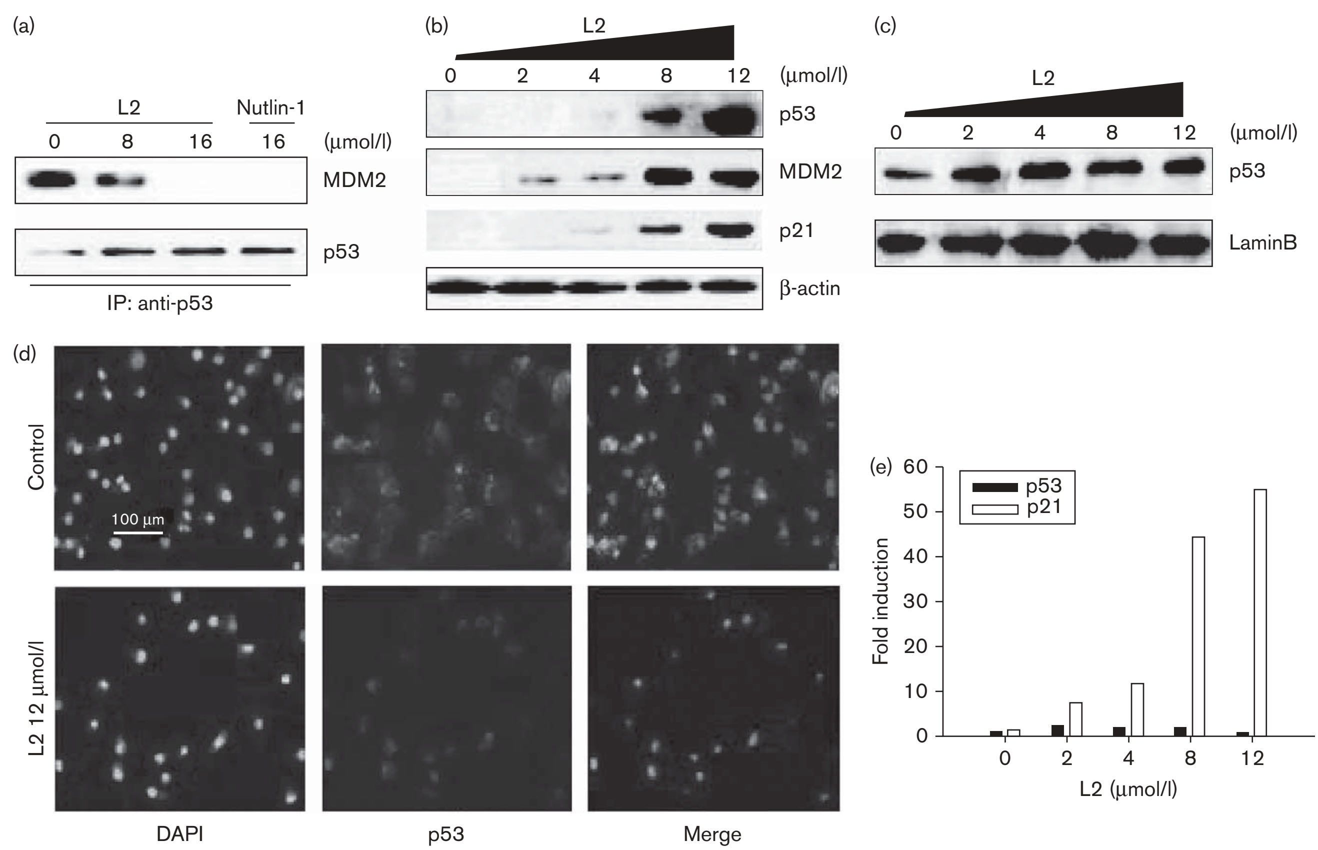

L2 blocked intracellular MDM2–p53 interaction, reactivated p53 in A549 cells by increasing its transcriptional activity, decreasing its degradation, and inhibiting its nuclear export. (a) A549 cells were treated with L2 (8 and 16 μmol/l) or nutlin-1 (16 μmol/l) for 48 h. MDM2 that combined with p53 was analyzed by immunoprecipitation. (b) A549 cells were incubated with the indicated concentrations of L2 for 48 h, and p53, MDM2, and p21 proteins were analyzed in the cell lysates by western blotting. (c) Extracted nucleoproteins and determined change of p53 protein in A549 cells treated with L2 for 48 h are shown. (d) A549 cells were incubated with 12 μmol/l L2 for 48 h and immunofluorescence studies revealed that p53 protein transferred from the cytoplasm to the nucleus. p53 was stained green after combination with anti-p53 antibody and cell nucleus were stained blue with DAPI (4′,6-diamidino-2-phenylindole). (e) A549 cells were treated with L2 for 48 h, Taqman real-time PCR assays were performed for detecting the mRNA levels of *p53* and *p21* genes. The results were expressed as fold induction compared with the untreated control. IP, immunoprecipitation.

L2 for 48 h (Fig. 2b). A similar result was observed at the protein level of p53 in the nucleus (Fig. 2c). We further investigated the exact reasons responsible for p53 stabilization by L2. After incubating A549 cells with 12 μmol/l L2 for 48 h, a large number of p53 proteins distributed from cytoplasm to nucleus were observed, which indicated that L2 could inhibit p53 protein export from the nucleus (Fig. 2d). In addition, as shown in Fig. 2e, we treated the A549 cells with L2 for 48 h and monitored the expressions of the *p53* and *p21* genes by real-time PCR. The p21 mRNA increased in a dose-dependent manner, reached up to 54.6-fold at the highest concentration (12 μmol/l) compared with the untreated control, whereas the *p53* gene expression was unaffected by L2. It showed that L2 upregulated p53 by means of posttranslational mechanisms. Taken together, these results showed that L2 could disrupt MDM2–p53 interaction, and stabilize p53 in A549 cells probably in three ways, one by increasing its transcriptional function, another by inhibiting its export from the nucleus, and the last one by reducing its degradation.

L2 induced cell cycle arrest in A549 and HL60 cells through different mechanisms

One of the main cellular consequences of p53 activation in proliferating cells was cell cycle arrest in G_0/G_1 and G_2/M phases. A549 cells were applied to investigate the effects of p53 stabilization on cell cycle progression after L2 treatments. It showed a dose-dependent reduction of the S-phase fraction in A549 cells after L2 treatments, with a maximal reduction of 28.64% at 8 μmol/l (Fig. 3a). Interestingly, cell cycle arrest could also be seen in HL60 cells after being treated with L2 (Fig. 3b). In A549 cells, G_2/M phase arrest occurred only at the highest concentration, whereas it was observed through all the concentrations in HL60 cells. However, there was no significant change in the S-phase fraction in HL60 cells. Originally, the mechanisms involved in this affair might

Fig. 3

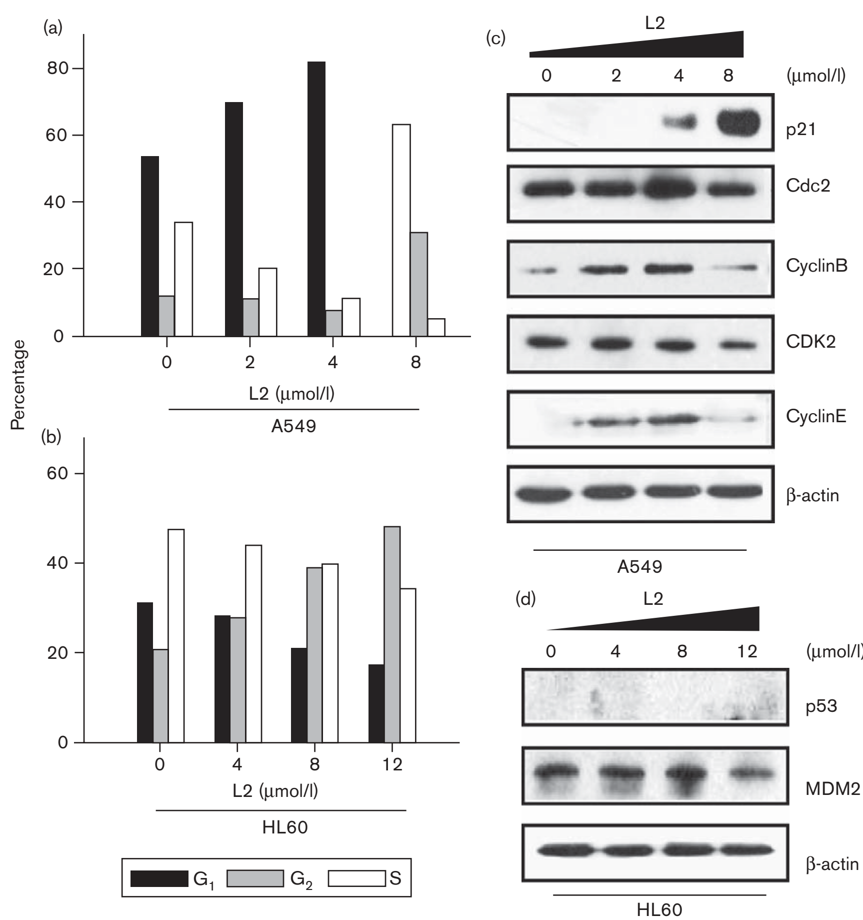

L2 induced cell cycle arrest in cells with wild-type or deleted *p53* (A549 and HL60), but the mechanisms involved in them were different. (a) A549 and HL60 cells were incubated with series of concentrations of L2 for 48 h, and cell cycle distributions were analyzed after propidium iodide staining, proportions of different phases were analyzed as in (a) and (b). (c) Some cell cycle related protein levels in A549 cells were analyzed by western blotting. (d) p53 and MDM2 levels in HL60 cells were analyzed by western blotting.

be different in the two cell lines. The cell cycle distribution changes in A549 cells were likely to be associated with a dose-dependent increase in the level of the cyclin-dependent kinase inhibitor p21, a known transcriptional target of p53 and also with the corresponding changes of its downstream proteins. Cdc2, cyclinB and cyclinE were upregulated at low concentrations (2 and 4 μmol/l) of L2 treatments and were downregulated at a high concentration (8 μmol/l), whereas CDK2 did not show significant changes except at a high concentration of L2 treatment in A549 cells (Fig. 3c). However, HL60 cells with *p53* deleted showed no significant changes in p53 and MDM2 (Fig. 3d). Therefore, we concluded that the p53 pathway might not be involved in cell cycle arrest in HL60 cells after L2 treatments. These data showed that L2 could cause cell cycle arrest through p53 pathway or other undiscovered mechanisms.

L2 induced A549 cells apoptosis through the activation of the p53 apoptotic pathway

To investigate whether apoptotic mechanisms were involved in L2-induced cell death, we stained A549 cells with Annexin–FITC and PI stain and measured the strength of fluorescence by flow cytometry. As shown in Fig. 4a, there was a concentration-dependent increase in the apoptotic ratio. The percentages of apoptosis reached up to 20.58, 34.47, and 68.78% at 4, 8, and 12 μmol/l L2 treatments in A549 cells, respectively (Fig. 4a). Apoptotic cells were morphologically evident with DAPI staining, and the presence of nuclear condensation and fragmentation was observed in 12 μmol/l L2-treated A549 cells (Fig. 4b). Furthermore, western blot analysis was performed to examine the possible mechanisms involved in p53-mediated cell death. As shown in Fig. 4c, a slight increase of Bax and decrease of Bcl-2 were observed 48 h after L2 treatments in A549 cells, which led to a significant increase in Bax/Bcl-2 ratio (Fig. 4d). Meanwhile, the expressions of XIAP, caspase8, caspase9, caspase3, and PARP were measured. As shown in Fig. 4e, L2 obviously decreased XIAP, caspase9, and caspase3 protein levels in a dose-dependent manner and it induced PARP to form cleaved fragments, whereas it had no visible effect on caspase8. In addition, A549 cells were exposed to 12 μmol/l of L2 for 1–8 h before staining with carboxy-DCFDA and analyzed by flow cytometry; a time-dependent increase in ROS content was observed (Fig. 4f). These results indicated that L2-induced apoptosis was caspase-dependent, and the mitochondrial pathway played a central role in this process.

Activation of p53 by L2 might be in a nongentoxic way

To confirm that the activation of p53 by L2 was dependent on its effect on MDM2, we, therefore, analyzed Ser^{20} phosphorylation in p53 from lysates of A549 cells treated with L2 and one positive genetoxic drug, etoposide. Western blot analysis revealed that etoposide caused phosphorylation of Ser^{20} in p53, but L2 did not. It suggested that activation of p53 by L2 was likely to be in a nongenotoxic mode and dependent on MDM2 (Fig. 5).

Discussion

The activities of oncogene *MDM2* and tumor suppressor gene *p53* are closely related to the development of cancer [16,17]. Earlier research shows that the growth or the death of the cells depends, to a large extent, on the fine-tuning of the MDM2–p53 interaction [16,17]. As MDM2 strictly controls the function of p53 at the posttranslational level, inhibition of the MDM2–p53 interaction allows an immediate p53-mediated response [6–8]. Compounds that prevent this interaction can be novel anticancer agents by activating the p53 pathway. Here, we found an ideal small-molecule candidate compound, which was the analog of nutlins, obtained a better antiproliferation effect on cancer cells compared with nutlin-1. We showed that the disruption of MDM2–p53 interaction by L2 resulted in the stabilization of p53 and the activation of the p53 pathway. Substantial cell cycle arrest and significant apoptotic cell death were observed and it further resulted in the reduction of cell mass and viability. Meanwhile, our data provided evidence that L2-induced stabilization of p53 was largely attributable to the decrease of protein degradation rather than the increase of its transcription level. In addition, different from most anticancer drugs, the activation of p53 by L2 was largely dependent on MDM2; therefore, a genetoxic mode was unlikely to be involved in the process. Surprisingly, L2 also showed a high antiproliferation effect on HL60 cells with *p53* deleted. It was concluded that L2 did not specifically target the p53–MDM2 interaction. It has been reported that MDM2 protein interacts with a large number of cellular proteins besides p53, and MDM2 is a pivotal molecule in tumor growth inducing both p53-dependent and p53-independent pathways. Considering E2F1, for example, MDM2 has been shown to interact with E2F1 and there is a striking similarity between one domain of E2F1 (amino acids 390–406) and the MDM2-binding domain of p53. Thus, on the basis of preliminary researches of other groups [10,11,18], we presumed that small-molecule p53–MDM 2-binding inhibitor, L2 had high antiproliferation effects on cells with nonfunctional *p53*, which could be attributed to some protein interaction with MDM2 instead of p53. Here we only discussed the activation of the p53 pathway by the activity of L2, leaving a large amount of unclear parts, which we would discover in the near future.

On the basis of the activation of the p53 pathway function, it was not surprising that L2 could induce cell cycle arrest and apoptosis. For the possible mechanisms responsible for L2-mediated cell cycle arrest of A549

Fig. 4

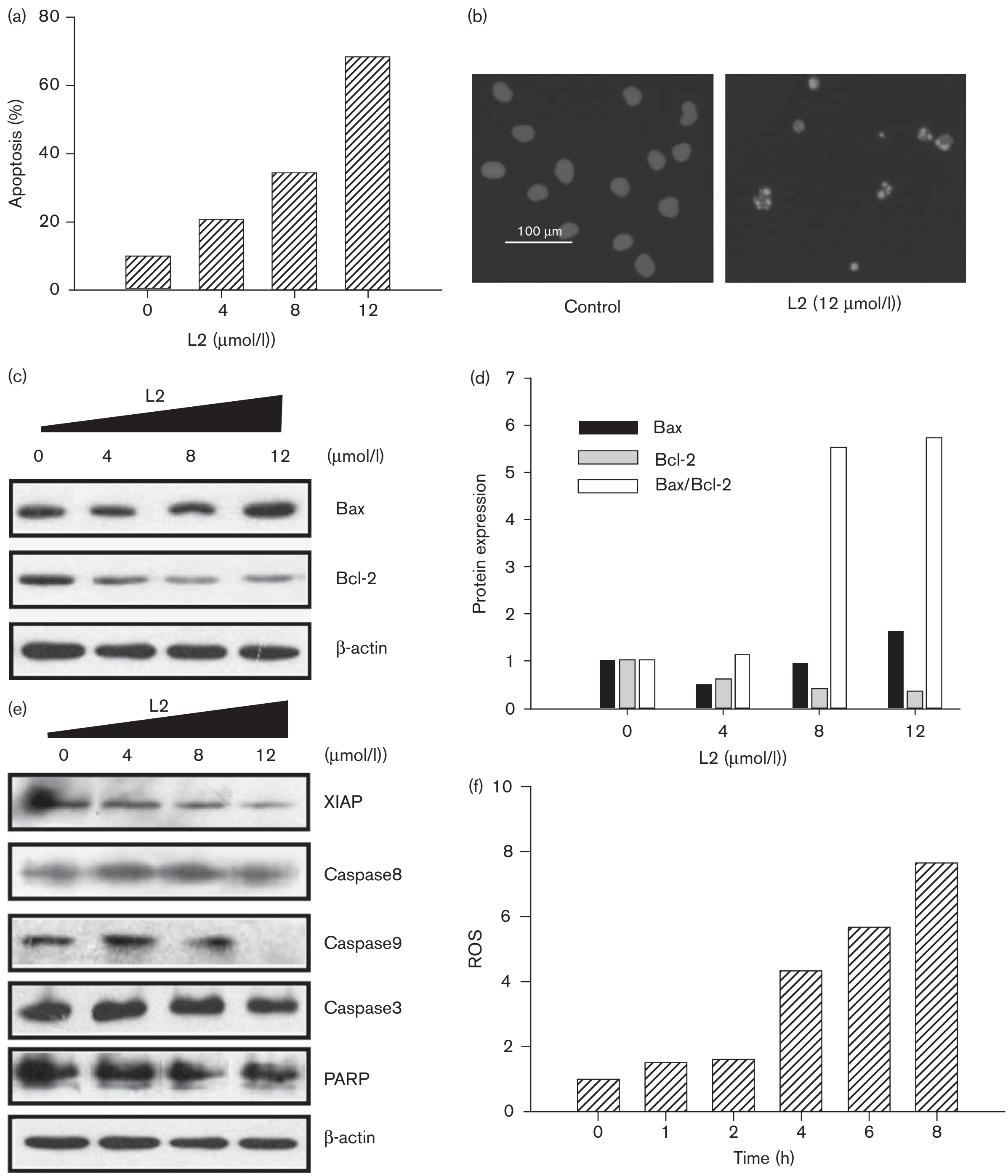

L2 activated the p53 pathway and induced apoptosis in A549 cells. (a) A549 cells were treated with L2 (4–12 μmol/l) or an equivalent amount of solvent (dimethyl sulfoxide) for 48 h, followed by analysis of apoptosis by flow cytometry with Annexin–FITC and propidium iodide staining. (b) A549 cells were stained with DAPI (4′,6-diamidino-2-phenylindole) after incubated with 12 μmol/l L2 for 48 h and the formations of apoptotic bodies could be clearly identified. (c) A549 cells were treated with L2 for 48 h, whole cell lysates were analyzed by western blotting. The decrease of Bcl-2 and the increase of Bax could be seen. (d) The significant increase of Bax/Bcl-2 ratio was shown. (e) The indicated concentrations of L2 decreased the accumulation of XIAP, caspase 9, and caspase 3 proteins and induced PARP to form cleaved fragments. No significant change was observed in caspase8 level. (f) L2 induced the A549 cells apoptosis accompanied by changes in reactive oxygen species (ROS). A549 cells were incubated with 12 μmol/l L2 for 0–8 h, and the content of ROS sustained increased.

Fig. 5

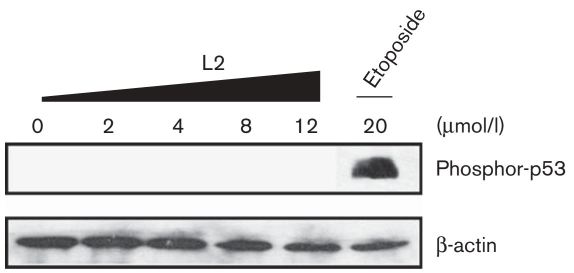

L2 was likely to activate the p53 pathway in a nongentoxic way. A549 cells were treated with L2 (2–12 μmol/l) or etoposide (20 μmol/l) for 48 h, and the amount of p53 phosphorylated on Ser^{20} was determined by western blotting in aliquots of cell lysates.

cells, we believed that the upregulated expression of *p21*, a p53 target gene, played a very important role in the whole process. It has been reported that as a protein kinase inhibitor, p21 has a vital role in the regulation of the cell cycle [19,20]. On the one hand, it can combine the complex of CDK2 and cyclinE, negatively regulate the G_1/S conversion, and prevent cells from entering the S phase [19,20,21]; on the other hand, it can inhibit the activity of Cdc2, leading to cell cycle arrest in the G_2 phase and blocking mitotic entry [19,20,22]. In our experiments, we found that L2 blocked the cell cycle in different phases with its different concentrations in A549 cells. Meanwhile the proportion of cells in S phase was reduced in a dose-dependent manner. Thus, that p21 strongly suppressed the activity of the CDK2–cyclinE complex might contribute to the G_0/G_1 phase arrest with the concentrations of 2 and 4 μmol/l, respectively, along with the accumulation of cyclinE later in a G_0/G_1 phase. Similarly, p21 directly inhibited the activity of Cdc2, which resulted in L2 arresting the cells at the G_2 phase and prevented them from entering mitosis at concentrations of 8 μmol/l. As was shown in Fig. 3a, L2 could also induce G_2/M phase arrest in HL60 cells, but there were no significant changes in the proportion of the S phase. By western blot analysis, no significant changes were observed in the protein levels of p53 and MDM2. It was shown that the mechanisms responsible for cell cycle arrest in A549 and HL60 cells after L2 treatment might be different. In cells with wild-type *p53*, cell cycle arrest might be related to the activation of the p53 pathway by L2; however, it might not be involved in cell cycle arrest in cells in which *p53* was deleted. We would devote further research to the issue.

Moreover, L2 could cause A549 cell apoptosis. It has been reported that the mitochondrial pathway plays an important role in the process of apoptosis and closely ties with the caspase cascade [23,24]. The final action is dependent on the balance between Bcl-2 and Bax and the increase of the Bax/Bcl-2 ratio can induce the release of cytochrome c from the mitochondria, which activates caspase3, leading to apoptosis [23–26]. In this study, we found that in A549 cells after L2 treatment, the ratio of Bax and Bcl-2 was changed. Bax acting as the targeted protein of the transcriptional factor p53 [27,28] increased, whereas the antiapoptotic protein family member, Bcl-2 [29,30], was on the contrary. The dramatic increase of the Bax/Bcl-2 ratio activated caspase cascade resulting in XIAP; Caspase9 and caspase3 reduced dose-dependently, and PARP, as a substrate of caspase3, formed cleaved fragments. There was no significant change in caspase8 level. We, therefore, concluded that the L2-induced apoptosis was caspase-dependent and the mitochondrial pathway played an important role in it. In addition, numerous investigations have indicated that ROS is a powerful activator of the loss of mitochondrial membrane potential and apoptosis [31,32], and current data show that cellular ROS can be modulated by p53 in a number of ways [33]. In our experiments, we found that ROS production was generated as time increased, showing that ROS took part in L2-caused apoptosis in A549 cells. In this process, we believed that the upregulation of p53 might be the inducible factor for the generation of ROS. Taken together, the mechanisms involved in the apoptosis triggered by L2 could be concluded as follows: the change of the Bax/Bcl-2 ratio and the generation of ROS allowing exit of some mitochondrial proteins, which activated caspase cascade, and finally led to apoptosis. So far, all our experiments indicated that compound L2 was a powerful apoptosis-inducing agent, which effectively widened the prospects for the development of L2.

In conclusion, as an effective inhibitor of MDM2–p53 interaction, L2 induced cell cycle arrest and apoptosis to achieve the purpose of inhibiting cell growth, and L2 stabilized p53 by increasing its transcriptional activity, inhibiting its export, and decreasing its degradation, which was a nongenetoxic process. We hope that the study of L2 can lay the foundation for its further development.

Acknowledgements

This study received financial support from the National Natural Science Foundation 30873163, the National Undergraduate Innovative Training Program 1094, and the Zhejiang Natural Science Foundation R2080326.

References

1 Braithwaite AW, Royds JA, Jackson P. The p53 story: layers of complexity. *Carcinogenesis* 2005; **26**:1161–1169.
2 Wawrzynow B, Zylicz A, Wallace M, Hupp T, Zylicz M. MDM2 chaperones the p53 tumor suppressor. *J Biol Chem* 2007; **282**:32603–32612.
3 Meek DW. The p53 response to DNA damage. *DNA Repair (Amst)* 2004; **3**:1049–1056.
4 Toledo F, Wahl GM. Regulating the p53 pathway: in vitro hypotheses, in vivo veritas. *Nat Rev Cancer* 2006; **6**:909–923.
5 Vousden KH, Lu X. Live or let die: the cell's response to p53. *Nat Rev Cancer* 2002; **2**:594–604.

6 Vassilev LT. MDM2 inhibitors for cancer therapy. *Trends Mol Med* 2007; **13**:23–31.
7 Bose I, Ghosh B. The p53-MDM2 network: from oscillations to apoptosis. *J Biosci* 2007; **32**:991–997.
8 Shu KX, Li B, Wu LX. The p53 network: p53 and its downstream genes. *Colloids Surf B Biointerfaces* 2007; **55**:10–18.
9 Tovar C, Rosinski J, Filipovic Z, Higgins B, Kolinsky K, Hilton H, *et al*. Small-molecule MDM2 antagonists reveal aberrant p53 signaling in cancer: implications for therapy. *Proc Natl Acad Sci U S A* 2006; **103**:1888–1893.
10 Ganguli G, Wasylyk B. p53-independent functions of MDM2. *Mol Cancer Res* 2003; **1**:1027–1035.
11 Zhang Z, Wang H, Li M, Rayburn ER, Agrawal S, Zhang R. Stabilization of E2F1 protein by MDM2 through the E2F1 ubiquitination pathway. *Oncogene* 2005; **24**:7238–7247.
12 Vassilev LT. Small-molecule antagonists of p53-MDM2 binding: research tools and potential therapeutics. *Cell Cycle* 2004; **3**:419–421.
13 Vassilev LT, Vu BT, Graves B, Carvajal D, Podlaski F, Filipovic Z, *et al*. In vivo activation of the p53 pathway by small-molecule antagonists of MDM2. *Science* 2004; **303**:844–848.
14 Vakifahmetoglu H, Olsson M, Orrenius S, Zhivotovsky B. Functional connection between p53 and caspase-2 is essential for apoptosis induced by DNA damage. *Oncogene* 2006; **25**:5683–5692.
15 Han S, Sidell N, Fisher PB, Roman J. Up-regulation of p21 gene expression by peroxisome proliferator-activated receptor gamma in human lung carcinoma cells. *Clin Cancer Res* 2004; **10**:1911–1919.
16 Haupt Y. p53 regulation: a family affair. *Cell Cycle* 2004; **3**:884–885.
17 Proctor CJ, Gray DA. Explaining oscillations and variability in the p53-Mdm2 system. *BMC Syst Biol* 2008; **2**:75.
18 Secchiero P, Zerbinati C, Melloni E, Milani D, Campioni D, Fadda R, *et al*. The MDM-2 antagonist nutlin-3 promotes the maturation of acute myeloid leukemic blasts. *Neoplasia* 2007; **9**:853–861.
19 Abukhdeir AM, Park BH. P21 and p27: roles in carcinogenesis and drug resistance. *Expert Rev Mol Med* 2008; **10**:e19.
20 Kumar R, Gururaj AE, Barnes CJ. p21-activated kinases in cancer. *Nat Rev Cancer* 2006; **6**:459–471.
21 Zhang LH, Youn HD, Liu JO. Inhibition of cell cycle progression by the novel cyclophilin ligand sanglifehrin A is mediated through the NFkappa B-dependent activation of p53. *J Biol Chem* 2001; **276**:43534–43540.
22 Lin YC, Wang FF. Mechanisms underlying the pro-survival pathway of p53 in suppressing mitotic death induced by adriamycin. *Cell Signal* 2008; **20**:258–267.
23 Ling YH, Liebes L, Zou Y, Perez-Soler R. Reactive oxygen species generation and mitochondrial dysfunction in the apoptotic response to Bortezomib, a novel proteasome inhibitor, in human H460 non-small cell lung cancer cells. *J Biol Chem* 2003; **278**:33714–33723.
24 Ryan L, O'Callaghan YC, O'Brien NM. The role of the mitochondria in apoptosis induced by 7 beta-hydroxycholesterol and cholesterol-5 beta, 6 beta-epoxide. *Br J Nutr* 2005; **94**:519–525.
25 Yamanaka K, Rocchi P, Miyake H, Fazli L, Vessella B, Zangemeister-Wittke U, Gleave ME. A novel antisense oligonucleotide inhibiting several antiapoptotic Bcl-2 family members induces apoptosis and enhances chemosensitivity in androgen-independent human prostate cancer PC3 cells. *Mol Cancer Ther* 2005; **4**:1689–1698.
26 Katiyar SK, Roy AM, Baliga MS. Silymarin induces apoptosis primarily through a p53-dependent pathway involving Bcl-2/Bax, cytochrome c release, and caspase activation. *Mol Cancer Ther* 2005; **4**:207–216.
27 Zhou X, Wang XW, Xu L, Hagiwara K, Nagashima M, Wolkowicz R, *et al*. COOH-terminal domain of p53 modulates p53-mediated transcriptional transactivation, cell growth, and apoptosis. *Cancer Res* 1999; **59**:843–848.
28 Basu A, Haldar S. The relationship between Bcl2, Bax and p53: consequences for cell cycle progression and cell death. *Mol Hum Reprod* 1998; **4**:1099–1109.
29 Sun J, Li ZM, Hu ZY, Lin XB, Zhou NN, Xian LJ, *et al*. ApoG2 inhibits antiapoptotic Bcl-2 family proteins and induces mitochondria-dependent apoptosis in human lymphoma U937 cells. *Anticancer Drugs* 2008; **19**:967–974.
30 Galluzzi L, Morselli E, Kepp O, Tajeddine N, Kroemer G. Targeting p53 to mitochondria for cancer therapy. *Cell Cycle* 2008; **7**: 1949–1955.
31 Gomez-Lazaro M, Galindo MF, Melero-Fernandez de Mera RM, Fernandez-Gómez FJ, Concannon CG, Segura MF, *et al*. Reactive oxygen species and p38 mitogen-activated protein kinase activate Bax to induce mitochondrial cytochrome c release and apoptosis in response to malonate. *Mol Pharmacol* 2007; **71**:736–743.
32 Ying M, Tu C, Ying H, Hu Y, He Q, Yang B. MSFTZ, a flavanone derivative, induces human hepatoma cell apoptosis via a reactive oxygen species- and caspase-dependent mitochondrial pathway. *J Pharmacol Exp Ther* 2008; **325**:758–765.
33 Liu B, Chen Y, St Clair DK. ROS and p53: a versatile partnership. *Free Radic Biol Med* 2008; **44**:1529–1535.